Solid-State Spun Fibers from 1 mm Long Carbon Nanotube Forests Synthesized by Water-Assisted Chemical Vapor Deposition

Shanju Zhang,[a] Lingbo Zhu,[b] Marilyn L. Minus,[a] Han Gi Chae,[a] Sudhakar Jagannathan,[a] Ching-Ping Wong,[b] Janusz Kowalik,[c] Luke B. Roberson,[d] and Satish Kumar*[a]

[a]*School of Polymer, Textile and Fiber Engineering, Georgia Institute of Technology, 801 Ferst Drive, Atlanta, Georgia 30332*

[b]*School of Materials Sciences and Engineering, Georgia Institute of Technology, 771 Ferst Drive, Atlanta, Georgia 30332*

[c]*School of Chemistry and Biochemistry, Georgia Institute of Technology, Atlanta GA 30332*

[d]*National Aeronautics and Space Administraion, John F. Kennedy Space Center, Kennedy Space Center, FL 32899*

* Email: shanju.zhang@ptfe.gatech.edu; satish.kumar@ptfe.gatech.edu

Abstract: In this work, we report continuous carbon nanotube fibers dry-drawn directly from water-assisted CVD grown forests with millimeter scale length. As-drawn nanotube fibers exist as aerogel and can be transformed into more compact fibers through twisting or densification with a volatile liquid. Nanotube fibers are characterized by scanning electron microscopy (SEM), X-ray photoelectron spectroscopy (XPS), Raman microscopy and wide-angle X-ray diffraction (WAXD). Mechanical behavior and electrical conductivity of the post-treated nanotube fibers are investigated.

Introduction

Carbon nanotubes (CNTs) are very promising candidates for the development of the next generation of high-performance, lightweight fibers and textiles with high modulus and strength. Breakthroughs have been made in coagulation spinning of single-walled (SWNTs) and multiwalled (MWNTs) nanotubes from polymer solution,[1-3] in gas-state spinning of SWNTs and MWNTs from reaction furnace,[4-6] in liquid crystalline wet spinning of SWNTs from super acids [7-9] as well as in solid-state spinning of MWNTs from vertically aligned nanotube forests.[10-13]

Water-assisted chemical vapor deposition (CVD) synthesis represents a novel and promising process for size-selective growth of highly pure, very long and vertically aligned CNT forests.[14-18] Millimeter long SWNTs,[14,15] MWNTs[16,17] and double-walled nanotubes (DWNTs)[18] have been reported by adding a small amount of water into the CVD chamber. Longer nanotubes are expected to provide efficient mechanical load transfer, as well as electron and phonon transport.[19]

In this work, we report continuous MWNT fibers dry-drawn from 1 mm long water-assisted CVD grown nanotube forests. The as-drawn fibers are twisted and subsequently densified to lock-in the effects from twisting. The mechanical and electrical properties of the post-treated fibers are investigated.

Experimental part

Water-assisted CVD synthesis was performed in a horizontal alumina tube (3.8 cm diameter; 92 cm long) housed in a Lindberg Blue furnace.[16,17] The substrates used in this study were (001) silicon wafers coated with 500 nm thermally grown SiO_2. The catalyst layers of Al_2O_3 (15 nm)/Fe (2 nm) were formed on the silicon wafer by sequential e-

beam evaporation. CVD growth of CNTs was carried out at 750 °C with ethylene (150 sccm) as the carbon source, and hydrogen (180 sccm) and argon (350 sccm) as carrier gases. The water vapor concentration in the CVD chamber was controlled at 775 ppm by bubbling a small amount of argon gas through water.

The nanotube fibers were produced from the MWNT forests by using tweezers to contact the side wall and then hand-drawn at a speed of approximately 50 cm/min. The as-drawn fibers were physically twisted using a motorized drive at 500 rpm. The twisted fibers were passed through ethanol to provide permanent twisting.

Morphology and microstructure of the fibers were studied using LEO 1530 scanning electron microscopy (SEM) at 5 kV and Hitachi HF-2000 transmission electron microscopy (TEM) at 200 kV. The cross-sections of the fibers were obtained using the microtoming technique. Raman spectra were collected in the back scattering geometry using Holoprobe Research Raman Microscope made by Kaiser Optical System using 785 nm excitation laser with polarizer. X-ray diffraction patterns were obtained on multifilament bundles on Rigaku Micromax-002 (λ = 0.15418 nm) using Rigaku R-axis IV ++ detection system. X-ray photoelectron spectroscopy (XPS) analysis was conducted on a model SSX-100 spectrometer (Surface Science Instruments).

The mechanical properties of the fibers were determined using RSA III solids analyzer (Rheometric Scientific, Co.) at room temperature. The displacement was determined by a controlled speed of 0.05 mm/min with a gauge length of 25 mm. For each fiber, at least 5 samples were tested.

Results and Discussion

Figure 1 shows SEM images of 1-mm high MWNT forest grown at 750 °C for 20 min. The MWNTs are 5 ~ 7 walls and ~ 10 nm in diameter. The nanotubes contain very little amorphous carbon based on the TEM images (inset in Figure 1a). A close examination of the forest under SEM reveals that the nanotubes are vertically aligned along the growth direction and form interconnected branches (Figure 1b, c and d). X-ray photoelectron spectroscopy (XPS) survey scans on the top and bottom of MWNT forests show only carbon (eV ~ 300) with the absence of iron catalysts (eV ~ 700, 950) (Figure 2). These results demonstrate that the as-grown MWNT forests are of high purity. The above unique structure of the nanotube forests with high purity, interconnected nanotube bundles as well as highly entangled network makes it possible to draw continuous fibers from the solid forests.[19]

The neat MWNT fibers in this work were hand-drawn from the MWNT forests using tweezers at approximately 50 cm/min (Figure 3). As-drawn fibers appeared as aerogel ribbons whose width and thickness were controlled by the forest sidewall width used for spinning fibers. The ribbon-like aerogel fibers spun from the 1-mm wide sidewall had width of ~ 80 μm and thickness of ~ 15 μm. About 1 m long CNT fibers were spun out for easy handling by hand, although there was no theoretical limit on the drawn length for this dry-drawing processing.

Figure 4a and b show SEM images of as-drawn nanotube fibers. The spacing between nanotubes in this aerogel fiber varies from tens of nm to hundreds of nm (Figure 4b). The as-drawn aerogel fibers easily stick to the surface of another object and therefore, it is difficult to handle them for most practical applications. We densified the as-drawn aerogel fibers by passing them through ethanol.[11,15] After ethanol evaporation, the aerogel

fibers densified into more compact fibers with width of ~ 10 μm and thickness of ~ 3 μm (Figure 4c and d).

Nanotube orientation in the fiber was studied using Raman microscopy. The Raman ratios $I_{G,0°} / I_{G,90°}$ was determined from the peak density of G-band at ca. 1590 cm^{-1} for polarization parallel and perpendicular to the fiber long axis. The values for as-drawn aerogel fiber and densified fiber were calculated to be 2.7 and 2.2, respectively (Figure 5), indicating a small decrease in nanotube orientation during densification.

The nanotube alignment in the densified fiber was also determined by wide angle X-ray diffraction (WAXD). A two-dimensional (2D) WAXD pattern shows Bragg diffraction on the equator at $2\theta = 25.5°$ (Figure 6a), corresponding to the graphite (002) plane in the CNTs. The calculated d spacing is 0.348 nm. This value is 0.007 nm larger than the previously reported value of 0.341 nm of arc-discharge or laser ablation produced MWNTs,[20] suggesting that the CVD produced MWNTs are somewhat more disordered. The crystal size deduced from (002) Bragg peak is ~ 2.0 nm, which is consistent with the TEM result of 5 ~ 7 walled MWNTs (inset of Figure 1a). The azimuthal scan of the (002) Bragg diffraction was obtained by plotting 2D data as intensity, I, versus azimuthal angle, ϕ (Figure 6b). The data was fitted using Lorentzian function and the fitted density was plotted in Figure 6b as a solid line. The full width at half-maximum (FWHM) of the Lorentzian function is 54.0°, indicating that the aligned nanotubes have a mosaic angle of ± 27.0 ° around the fiber axis. The degree of alignment of the nanotubes was estimated from the orientational order parameter proposed by Hermanns. The order parameter is defined by $s = (3\langle\cos^2\varphi\rangle - 1)/2$, where $\langle\varphi\rangle$ denotes the average angle between the nanotube direction and the fiber axis. The value of the order parameter s was derived to

be 0.19 from the azimuthal intensity distribution. Note that for a perfect orientation of the lattice plane with its normal in the plane of equator, the orientational order parameter would be $s = 1.0$. The relative low nanotube orientation in this work implies that there is significant room for improving in tensile modulus of the fibers.[21]

It has been reported that twising significantly enhances the stress transfer between nanotubes under the aforementioned tensile forces.[22,23] However, the twisted CNT fibers were not stable and tended to relax (untwist and coil) under unconstrained environments.[24] Twisted CNT fibers were passed through ethanol and effectively stabilized after complete ethanol evaporation (Figure 7). The twisted nanotube fibers after densification were very flexible and non-adhesive. They were easily handled and manipulated (Figure 7 c and d).

Mechanical performance of the MWNT fibers was studied by analyzing the stress-strain curves. The stress-strain curves were obtained by dividing the force by cross section area, which was measured from SEM images (Figure 8). Figure 9 shows the typical stress-strain curves of densified fiber (D), twisted fiber (T) and twisted fiber with densification (T&D fiber). The D nanotube fibers were broken at $2.2 \pm 0.2\%$ with 0.35 ± 0.07 GPa tensile strength and 25 ± 5 GPa Young's modulus (Table 1). The relative low value of Young's modulus is attributed to the low degree of nanotube alignments in the fiber as discussed above. Increasing the nanotube orientation could significantly enhance the Young's modulus.[21] With twisting, tensile strength increased and Young's modulus decreased which are expected because of efficient load transfer and reduction of nanotube orientation.[25] Twisting increased the strain-to-failure, resulting in the enhanced fiber toughness. The toughness of T&D nanotube fibers are $\sim 30 \pm 4$ J/g, which is 500% higher

than those (~ 5 ± 1 J/g) of D nanotube fibers (Table 1). It is interesting to note that the T&D nanotube fibers exhibit two linear regions, which correspond to two values of Young's modulus. The low modulus initial region is due to high twisting. After the initial region, the Young's modulus of the fibers increases ~ 100 %. It is assumed that this process corresponds to re-orientation of the nanotubes in the fibers during the stretching and is analogous to the effect of post-drawing on the performance of the as-spun polymer fibers.[26]

The electrical conductivities of the densified nanotube fibers were measured along the fiber axis using two-point probes under the direct current (DC) resource. The current-voltage (*I-V*) curve of the MWNT fiber is linear (Figure 9) with axial conductivity at room temperature of ~ 5.0×10^4 $S \cdot m^{-1}$. This result can be favorably compared to the previous reported value of 3.0×10^4 $S \cdot m^{-1}$ for the dry-drawn MWNT fibers.[12] The somewhat higher electrical conductivity of the MWNT fiber in this work may be attributed to longer nanotubes.[27,28]

Conclusions

In conclusion, we have reported that 1 mm long water-assisted CVD grown carbon nanotubes can be directly dry-drawn into macroscopically continuous nanotube fibers. As-drawn nanotube fibers are aerogel and can be transformed into more compact fibers by twisting or passing through ethanol. We observe that the ethanol can stabilize the twisting effect. The resultant fibers have 500% higher toughness than those of only densified fibers. As water-assisted CVD can selectively grow long SWNTs, DWNTs and MWNTs with controlled diameters, this work should provide further encouragement to dry-drawn carbon nanotube fibers and sheets from different types of nanotube forests.

Acknowledgements

Financial support from the Air Force Office of Scientific Research (FA9550-06-1-0315) and from the National Aeronautics and Space Administration (UCF-FY-04) are gratefully appreciated.

References

1. B. Vigolo, A. Penicaud, C. Coulon, C. Sauder, R. Pailer, C. Journet, P. Bernier, P. Poulin, *Science,* 2000, **290**, 1331.
2. A. B. Dalton, S. Collins, E. Munoz, J. M. Razal, V. H. Ebron, J. P. Ferraris, J. N. Coleman, B. G. Kim, R. H. Baughman, *Nature, 2003,* **423**, 703.
3. P. Miaudet, S. Badaire, M. Maugey, A. Derre, V. Pichot, P. Launois, P. Poulin, C. Zakri, *Nano Lett.*, 2005, **5**, 2212.
4. H. W. Zhu, C. L. Xu, D. H. Wu, B. Q. Wei, R. Vajtai, P. M. Ajayan, *Science,*2002, **296**, 884.
5. Y. L. Li, I. A. Kinloch, A. H. Windle, *Science*, 2004, **304**, 276.
6. M. Motta, Y. L. Li, I. Kinloch, A. Windle, *Nano Lett.,* 2005, **5,** 1529.
7. L. M. Ericson, H. Fan, H. Peng, V. A. Davis, W. Zhou, J. Sulpizio, Y. Wang, R. Booker, J. Vavro, C. Guthy, A. N. G. Parra-Vasquez, M. J. Kim, S. Ramesh, R. K. Saini, C. Kittrell, G. Lavin, H. Schmidt, W. W. Adams, W. E. Billups, M. Pasquali, W. F. Hwang, R. H. Hauge, J. E. Fischer, R. E. Smalley, *Science,* 2004, **305**, 1447.
8. V. A. Davis, L. M. Ericson, A. N. G. Parra-Vasquez, H. Fan, Y. Wang, V. Prieto, J. A. Longoria, S. Ramesh, R. K. Saini, C. Kittrell, W. E. Billups, W. W. Adams, R. H. Hauge, R. E. Smalley, M. Pasquali, *Macromolecules,* 2004, **37**, 154.
9. Y. H. Wang, L. M. Ericson, C. Kittrell, M. J. Kim, H. W. Shan, H. Fan, S. Ripley, S. Ramesh, R. H. Hauge, W. W. Adam, M. Pasquali, R. E., Smalley, *Chem. Mater.,* 2005, **17**, 6361.
10. K. L. Jiang, Q. Q. Li, S. S. Fan, *Nature*, 2002, **419**, 801.

11. X. B. Zhang, K. L. Jiang, C. Feng, P. Liu, L. Zhang, J. Kong, T. H. Zhang, Q. Q. Li, S. S. Fan, *Adv. Mater.*, 2006, **18**, 1505.

12. M. Zhang, K. R. Atkinson, R. H. Baughman, *Science*, 2004, **306**, 1358.

13. X. Zhang, Q. Li, Y. Tu, Y. Li, J. Y. Coulter, L. Zheng, Y. Zhao, Q. Jia, D. E. Peterson, Y. Zhu, *Small*, 2007, **3**, 244.

14. K. Hata, D. N. Futaba, K. Mizuno, T. Namai, M. Ymura, S. Iijima, *Science*, 2004, **306**, 1362.

15. D. N. Futaba, K. Hata, T. Yamada, T. Hiraoka, Y. Hayamizu, Y. Kakudate, O. Tanaike, H. Hatori, M. Yumura, S. Iijima, *Nat. Mater.*,2006, **5**, 987.

16. L. B. Zhu, Y. H. Xiu, D. W. Hess, C. P. Wong, *Nano. Lett.*, 2005, **5**, 2641.

17. L. B. Zhu, Y. Y. Sun, D. W. Hess, C. P. Wong, *Nano Lett.*,2006, **6**: 243.

18. T. Yamada, T. Namai, K. Hata, D. N. Futaba, K. Mizuno, J. Fan, M. Yudasaka, M. Yumura, S. Iijima, *Nature Nanotech.* 2006, **1**, 131.

19. R. H. Baughman, *Nature Nanotech.*, 2006, **1**, 94.

20. L.Lin, C. Bower, O. Zhou, *Appl. Phys. Lett.*, 1998, **73**, 1197.

21. T. Liu, S. Kumar, *Nano Lett.*, 2003, **3**, 647.

22. D. Qian, W. K. Liu, R. S. Ruoff, *Compos. Sci. Technol.*, 2003, **63**, 1561.

23. R. B. Pipes, P. Hubert, *Compos. Sci. Technol.*, 2002, **62**, 419.

24. P. Bradford, S. Fang, M. Zhang, R. H. Baughman, *SAMPE J.,* 2007 **43,** 2.

25. J. W. S. Hearle, P. Grosberg, S. Backer, *Structural mechanics of fibers, yarns and fabrics*, Wiley, New York, 1969, **vol. 1**.

26. H. G. Chae, M. L. Minus, S. Kumar, *Polymer*, 2006, **47**, 3494.

27. D. Hecht, L. Hu, G. Gruner, *Appl. Phys. Lett.*, 2006, **89**, 133112.

28. I. Balberg, N. Binenbaum, C. H. Anderson, *Phys. Rev. Lett.*, 1983, **51**, 16056.

Table 1 Data of mechanical properties for the post-treated dry-drawn carbon nanotube fibers

Samples	Strength(GPa)	Modulus(GPa)	Elongation(%)	Toughness(J/g)
D-fibers	0.35 ± 0.07	25 ± 5	2.2 ± 0.2	5 ± 1
T-fibers	0.40 ± 0.08	10 ± 2	5.0 ± 1.0	11 ± 2
T & D- fibers	0.50 ± 0.10	4.0 ± 0.5/ 8.0 ± 1.0	11.0 ± 3.0	30 ± 4

FIGURE CAPTIONS

Figure 1 SEM images of a MWNT forest for fiber spinning: a) 1 mm high vertically standing MWNT forest grown by water-assisted CVD growth. Inset, high resolution TEM image of an individual nanotube. b) Forest wall. The circle shows aligned CNTs with entangled branches. c) and d) Top and bottom of the forest. The circles reveal entangled network.

Figure 2 XPS survey scans of top and bottom of the nanotube forest.

Figure 3 Spinning continuous MWNT fibers from the forest: a) Photograph of the fiber in the process of being drawn from the 10×10 mm^2 wafer scale forest; b) optical image showing the nanotubes being pulled from the forest wall into a fiber.

Figure 4 SEM images of neat MWNT fibers: a) As-drawn aerogel fiber; b) nanotube arrangements in the as-drawn fiber; c) densified fiber and d) nanotube arrangement in the desified fiber.

Figure 5 Raman G-band spectra for (a) as-drawn aerogel fiber and (b) densified fiber. The angle between polarizer and the fiber axis are 0 ° and 90 °.

Figure 6 (a) WAXD patterns of densified MWNT filaments. (B) The azimuthal intensity scanning of the (002) reflection and its Lorentzian fit overlaid on the azimuthal intensity

data. Dots represent the experimental data and the solid line corresponds to the Lorentzian fit.

Figure 7 SEM images of twisted fibers with densification: (a) single fiber; (b) nanotube arrangement in the fiber; (c) nanotube fiber knot and (d) double twisted fiber. Dotted arrow shows the fiber axis and solid arrow shows the direction of nanotube orientation. There is an angle between them due to twisting.

Figure 8 SEM images of cross-sections: (a) densified fiber and (b) twisted fiber.

Figure 9 Stress-strain curves of different MWNT fibers: densified fiber (D-fiber), twisted fiber (T-fiber) and twisted fiber with densification (T&D fiber).

Figure 10 Current (I)-voltage (V) plot of a densified MWNT fiber.

Zhang et al. Figure 1

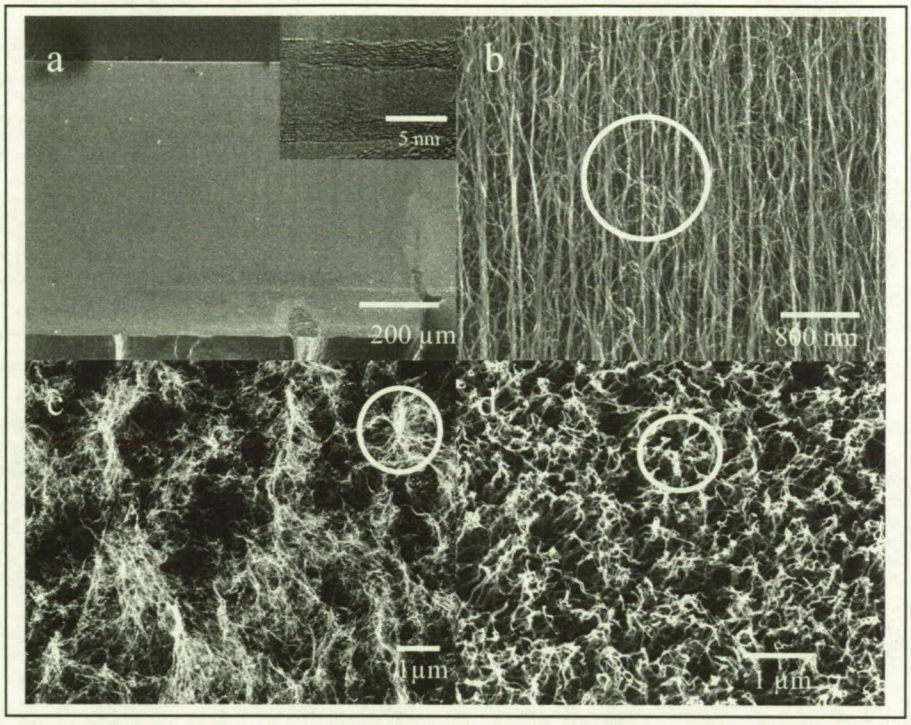

Zhang et al. Figure 2

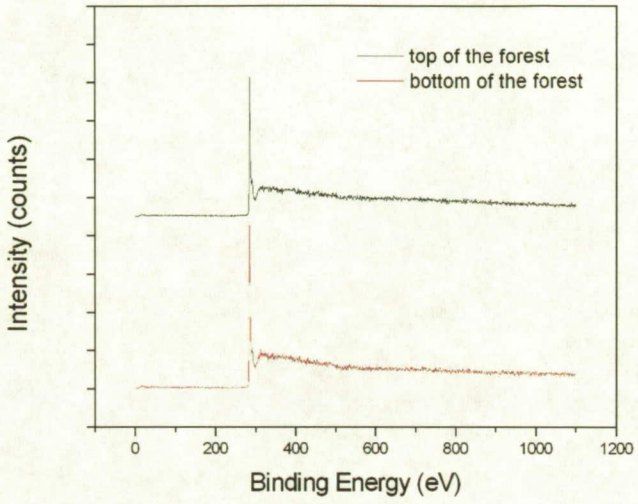

Zhang et al. Figure 3

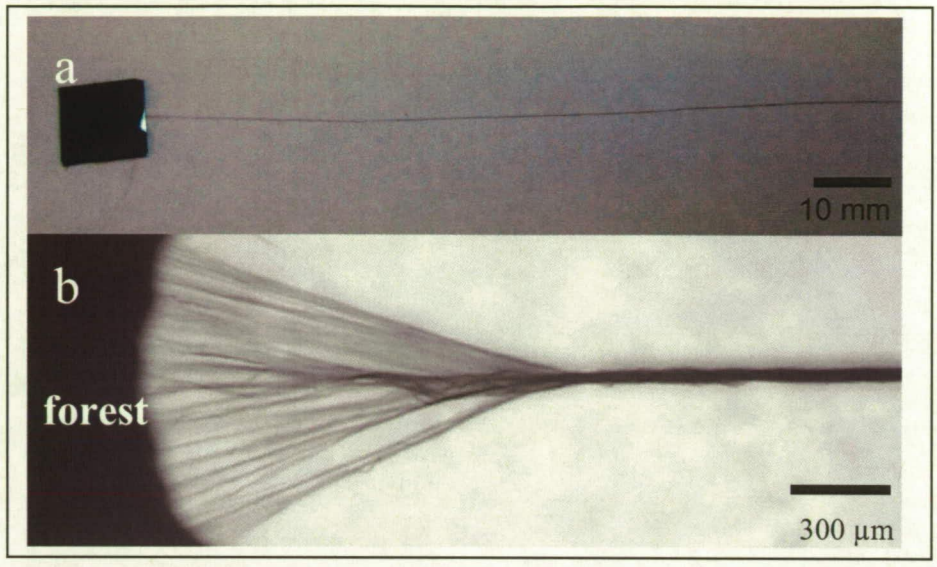

Zhang et al. Figure 4

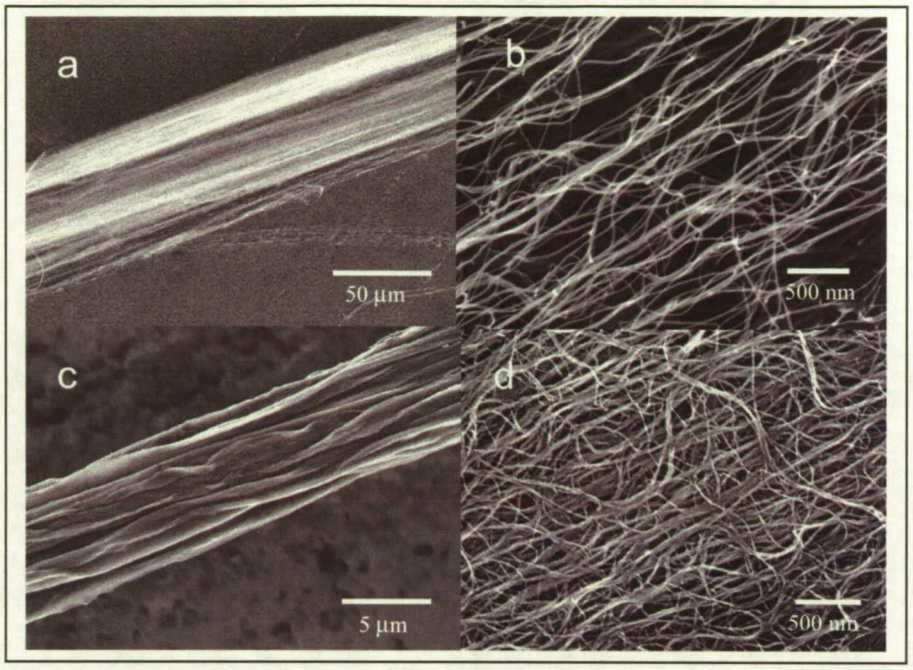

Zhang et al. Figure 5

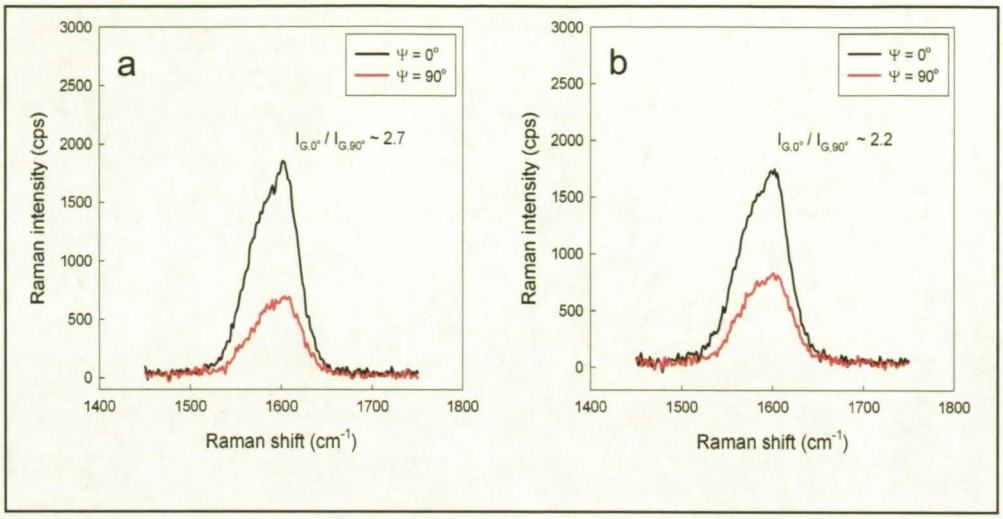

Zhang et al. Figure 6

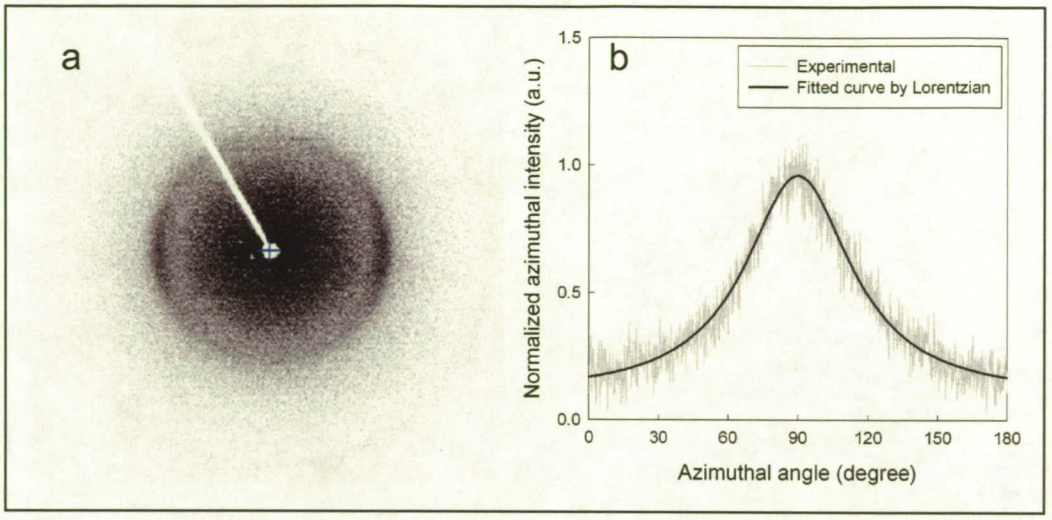

Zhang et al. Figure 7

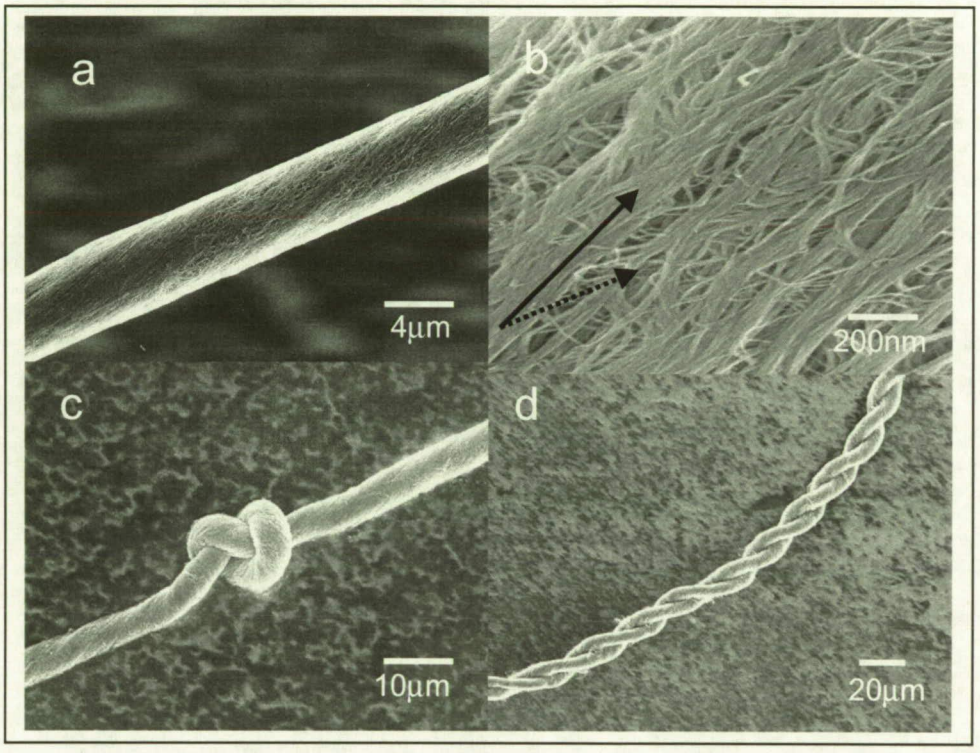

Zhang et al. Figure 8

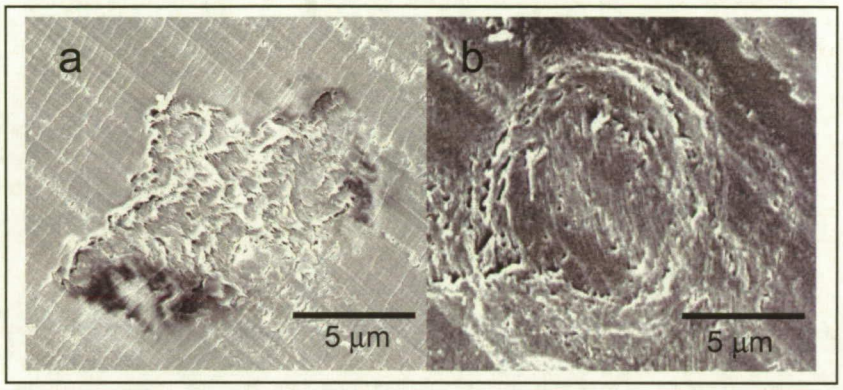

Zhang et al. Figure 9

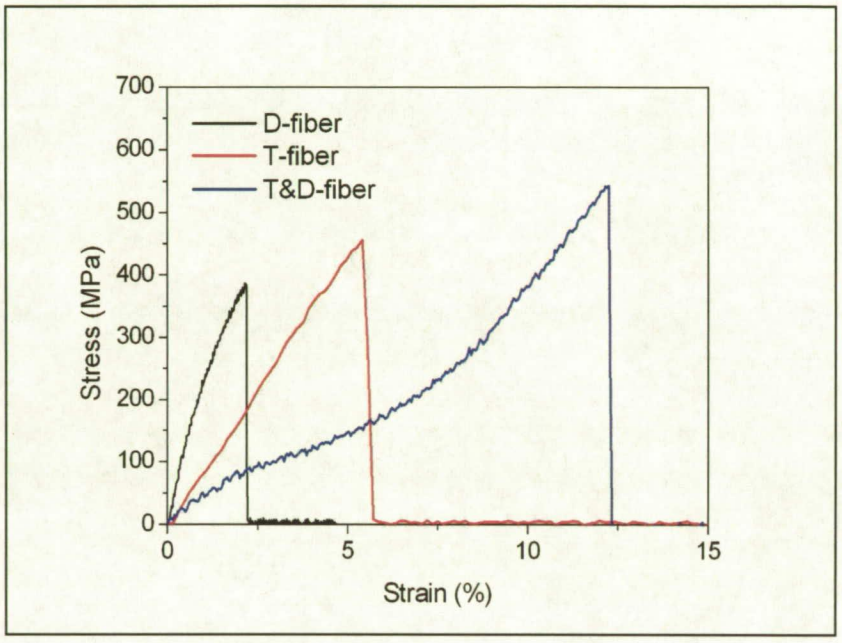

Zhang et al. Figure 10